

Figure 11 The measured radiation using Labvolt for the setup with the superstrate. [Color figure can be viewed in the online issue, which is available at wileyonlinelibrary.com]

dielectric constant ϵ_r of the medium, a new resonance frequency of 600 MHz is obtained.

A series of simulations reducing the antenna length and the superstrate distance cover are achieved until the resonant frequency of 1 GHz is obtained again. Ray optics, Snell law, and transmission line equivalence indicates that rays can be bent by the substrates in a suitable direction to adjust the gain. A series of practical experiments reproduces the gain and the return loss behavior obtained in simulations. Then, a new antenna loop with similar return loss and gain of a free space loop but 61% of length reduction is realized. Besides, the *E*-plane and *H*-plane pattern diagram also similar to the free space large loop antennas.

Another interesting consideration is the reduced length used in the transmission line equivalent model in axis AA' indicated in Figure 2. In general, $(\lambda/4)$ length models are used. In general, $(\lambda/4)$ models are used [5–7].

Finally, it is important to mention that to use the substrate multilayer structure to reduce antennas dimensions and recover the original gain, to the authors knowledge, has not been reported.

New development using other kind of antennas and other substrates are being studied aiming a dramatic size reduction and gain enhancement in wireless frequencies of 2.4 and 5 GHz.

ACKNOWLEDGMENT

The authors wish to thank CNPq for the grant to this research and Agilent for support of the ADS program as also ESSS for support of HFSS and Antenna Design Kit. One of the authors, Jorge Mitrione wishes to thank ROGERS Corporation to supply the laminates for this research.

REFERENCES

- L.C. Bahiana, M.S. Assis, and M.M. Rabello, *Antenas*, vol. 1, CETUC PUC-Rio.
- R. Schmitt, *Electromagnetics explained—A handbook for wireless/RF, EMC and high speed electronics*, 1st ed., Newnes, 2002.
- C.A. Balanis, *Antenna theory*, 3rd ed., Wiley, Hoboken, NJ, 2011.
- R.E. Collin, *Foundations for microwave engineering*, 2nd ed., Wiley, Hoboken, NJ, 2005.
- C.S. Lin, J.H. Shi, S.S. Zhong, Y. Wang, Gain enhancement technique for microstrip antennas, In: *Antennas and Propagation Society International Symposium*, San Jose, CA, 26–30 June 1989.
- H.Y. Yang, N.G. Alexopoulos, Gain enhancement methods for printed circuit antennas through multiple superstrates, *IEEE Trans Antennas Propag* 35 (1987).
- D.R. Jackson, N.G. Alexopoulos, Gain enhancement methods for printed circuit antennas, *IEEE Trans Antennas Propag* 33 (1985).
- Minicircuits, Application note on transformers, Application Note AN20-002.
- J. Huang, A review of antenna miniaturization techniques for wireless applications. Available at <http://trs-new.jpl.nasa.gov/dspace/bitstream/2014/12385/1/01-0484.pdf>
- T.K. Lo, C.O. Ho, Y. Hwang, E.K.W. Lam, B. Lee, Miniature aperture-coupled microstrip antenna of very high permittivity, *IEEE Electron Lett* 33 (1997).

© 2015 Wiley Periodicals, Inc.

SMALL-SIZE TWO-BRANCH MONOPOLE ANTENNA WITH INTEGRATED WIDEBAND MATCHING NETWORK FOR LTE TABLET COMPUTER

Kin-Lu Wong and Shan-Ni Hsu

Department of Electrical Engineering, National Sun Yat-sen University, Kaohsiung 80424, Taiwan; Corresponding author: wongkl@ema.ee.nsysu.edu.tw

Received 5 June 2014

ABSTRACT: A simple two-branch monopole antenna with an integrated wideband matching network to achieve the LTE dual-wideband operation (698–960/1710–2690 MHz) with a small occupied volume ($10 \times 30 \times 3 \text{ mm}^3$) in the tablet computer is presented. The two-branch monopole contributes to one resonant mode in the LTE low band and one resonant mode in the LTE high band. With the aid of the wideband matching network, the bandwidths of the two resonant modes can both be widened to cover the LTE dual-wideband operation. In addition, the matching network requires no additional board space on the system circuit board of the tablet computer and is disposed inside the ground clearance region occupied by the antenna. This makes it attractive for practical applications. Working principle of the wideband matching network on achieving the antenna's dual-wideband operation is described in this study. The antenna is also fabricated and tested. Experimental results are presented and discussed. © 2015 Wiley Periodicals, Inc. *Microwave Opt Technol Lett* 57:507–513, 2015; View this article online at wileyonlinelibrary.com. DOI 10.1002/mop.28876

Key words: mobile antennas; tablet computer antennas; LTE antennas; wideband matching network; small-size antennas

1. INTRODUCTION

It has been very challenging to achieve small size yet dual-wideband operation for the embedded antenna in the terminal communication device to achieve the LTE operation in the 698–960 and 1710–2690 MHz bands [1]. Although there have been many tablet computer antennas reported to cover the LTE dual-

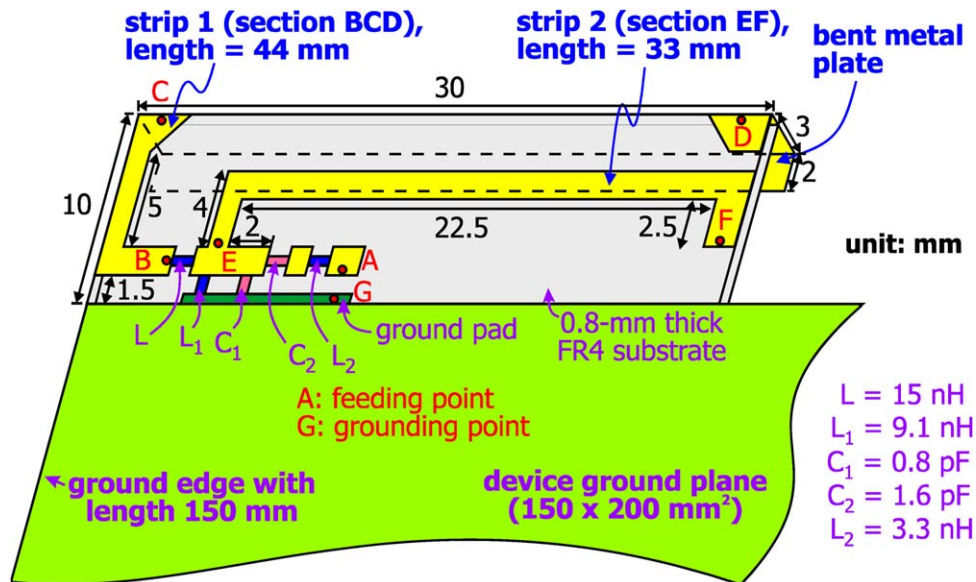


Figure 1 Geometry of the small-size two-branch monopole antenna with an integrated wideband matching network for the LTE tablet computer. [Color figure can be viewed in the online issue, which is available at wileyonlinelibrary.com]

wideband operation, the antenna structure is usually complicated and the required ground clearance is generally large [2–15]. Very few of the reported antennas can occupy a small ground clearance of about $10 \times 30 \text{ mm}^2$ only [15], if no active switching network is applied [14]. The recently reported LTE antenna in [15] uses two hybrid feeds and requires a small ground clearance of $10 \times 30 \text{ mm}^2$ and a thin thickness of 3.8 mm. The antenna uses a simple radiating metal plate to achieve a simple antenna structure. The dual-band operation is mainly obtained by a direct feed for the low band and a gap-coupled feed for the high band. To cover the LTE dual-wideband operation, two wideband matching networks are connected to the two hybrid feeds to greatly widen the antenna bandwidths. In such an antenna design with a small occupied ground clearance and a simple antenna structure, the wideband matching networks are crucial in achieving two wide operating bands for the LTE operation [15]. Hence, if the wideband matching network design can be simplified, it is expected that such an antenna design can be more attractive for practical applications.

In this article, we present a simple two-branch monopole antenna with an integrated wideband matching network to achieve the LTE dual-wideband operation (698–960/1710–2690 MHz) with a small occupied volume ($10 \times 30 \times 3 \text{ mm}^3$) in the tablet computer. In the proposed design, only one wideband matching network is required to achieve the LTE dual-wideband operation, which is simpler than the design reported in [15]. Also, the proposed design has a simple antenna structure, and the antenna’s occupied volume is small as well.

In this study, the two-branch monopole in the proposed design contributes to one resonant mode in the LTE low band and one resonant mode in the LTE high band. The wideband matching network formed by a shunt inductor, a shunt capacitor, a series capacitor, and a series inductor can lead to additional resonances occurred close to the two resonant modes contributed by the two-branch monopole. This behavior greatly widens the antenna’s low-band and high-band bandwidths, so that the desired LTE dual-wideband operation can be covered. Design considerations of the proposed antenna are described. Working principle of the wideband matching network on achieving the

dual-wideband operation for the antenna is addressed. Experimental results of the fabricated antenna are also presented and discussed.

2. PROPOSED ANTENNA

2.1. Antenna Structure

Figure 1 shows the geometry of the two-branch monopole antenna with an integrated wideband matching network for the LTE tablet computer. To show the proposed antenna more

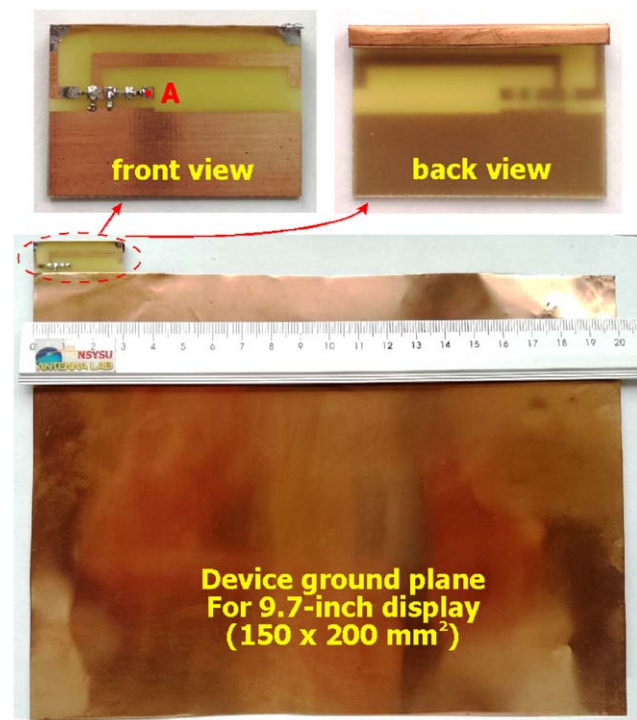


Figure 2 Photos of the fabricated antenna. [Color figure can be viewed in the online issue, which is available at wileyonlinelibrary.com]

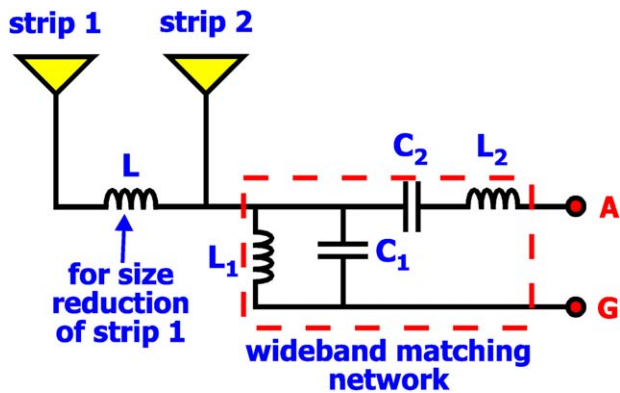


Figure 3 Simplified model of the antenna with the wideband matching network. [Color figure can be viewed in the online issue, which is available at wileyonlinelibrary.com]

clearly for understanding, the photos of the fabricated antenna are shown in Figure 2. The antenna is mounted along the long edge of the device ground plane of a tablet computer and flushed to one corner thereof. The dimensions of the device ground plane are selected to be $200 \times 150 \text{ mm}^2$ to fit for a 9.7-inch tablet computer, which is very popular on the market. In the experiment, the device ground plane is cut from a 0.2-mm thick copper plate.

The antenna occupies a ground clearance of $10 \times 30 \text{ mm}^2$ above the long edge of the device ground plane. The antenna comprises a two-branch monopole and a wideband matching network, both disposed on a 0.8-mm thick FR4 substrate of size $10 \times 30 \text{ mm}^2$, relative permittivity 4.4, and loss tangent 0.024. The two-branch monopole includes strip 1 (section BCD, length 42 mm) and strip 2 (section EF, length 33 mm), with strip 2 printed on the FR4 substrate and strip 1 connected to strip 2 through a chip inductor L of 15 nH. With the aid of the inductor L , which compensates for large capacitance of strip 1 at lower frequencies [16–19], strip 1 can contribute a resonant mode at about 800 MHz in the LTE low band. This leads to a small size for the antenna operated in the LTE low band. Also note that the major portion of strip 1 is mainly formed by a bent metal plate of $2 \times 3 \times 30 \text{ mm}^3$ connected to point C and D on the FR4 substrate. The bent metal plate can lead to a widened bandwidth of the excited resonant mode contributed by strip 1, although the obtained bandwidth is still far from covering the entire LTE low band.

Strip 2 is printed on the FR4 substrate and has a length of 33 mm, which is close to about 0.25 wavelength at about 2.2 GHz. Hence, the contributed resonant mode of strip 2 can easily be excited in the LTE high band. However, the bandwidth of the contributed resonant mode of strip 2 is also much less than that required for covering the LTE high band. In this case, without the wideband matching network, the antenna's low-band and high-band bandwidths are far from covering the LTE dual-wideband operation (698–960/1710–2690 MHz bands).

To aid in analyzing the antenna's dual-wideband operation, a simplified model of the antenna with the wideband matching network is shown in Figure 3. The wideband matching network includes a shunt chip inductor L_1 (9.1 nH), a shunt chip capacitor C_1 (0.8 pF), a series chip capacitor C_2 (1.6 pF) and a series chip inductor L_2 (3.3 nH). The inductor L_1 and capacitor C_2 can lead to significant bandwidth enhancement of the antenna's low band, with small effects on the high-band performance. Con-

versely, the capacitor C_1 and inductor L_2 can effectively adjust the impedance matching of the antenna's high band to achieve a much wider operating band, with small effects on the low-band performance. The wideband matching network can make it easy and convenient in achieving a dual-wideband operation for the proposed antenna. The working principle of the proposed antenna and its wideband matching network on achieving the antenna's dual-wideband operation is presented in the next subsection.

2.2. Working Principle

The proposed antenna can be decomposed into a low-band antenna (the case without strip 2) and a high-band antenna (the case without strip 1). Their corresponding geometries are shown in Figure 4. Note that in both the low-band and high-band antennas, the wideband matching network is present. Results of the simulated return loss for the proposed antenna, the low-band antenna, and the high-band antenna are presented in the figure. The simulated results are obtained using the full-wave electromagnetic field simulator HFSS version 15 [20]. The shaded frequency ranges denote the desired LTE low band and high band. It can be seen that strip 1 and strip 2, respectively, control the antenna's low band and high band. More specifically, strip 1 and strip 2 respectively contribute a resonant mode to the antenna's low band and high band, while the wideband matching network leads to bandwidth enhancement of the two operating bands at the same time. It is also noted that the proposed antenna can cover the desired LTE dual-wideband operation. Although the return loss at some frequencies in the low band is slightly less than 6 dB, the obtained antenna efficiencies including the mismatching losses are better than about 50%, which is acceptable for practical applications [2–15]. Results of the antenna efficiencies will be discussed with the aid of Figure 11 in Section 3.

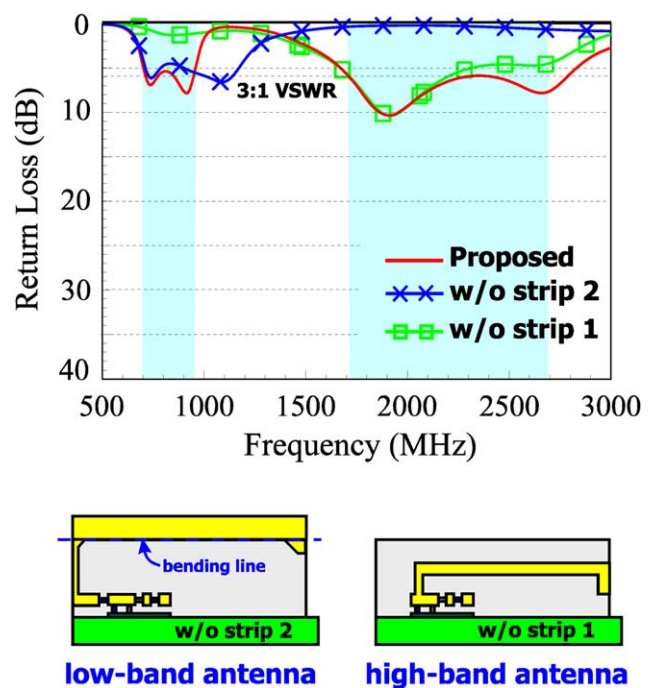


Figure 4 Simulated return loss for the proposed antenna, the case without strip 2 (low-band antenna), and the case without strip 1 (high-band antenna). [Color figure can be viewed in the online issue, which is available at wileyonlinelibrary.com]

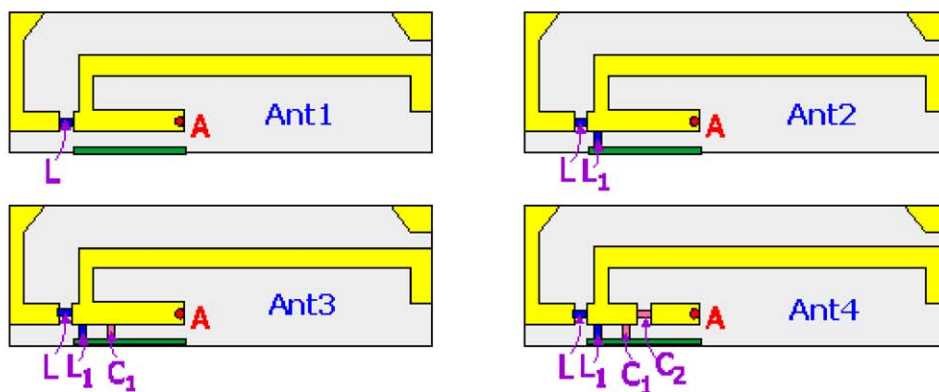
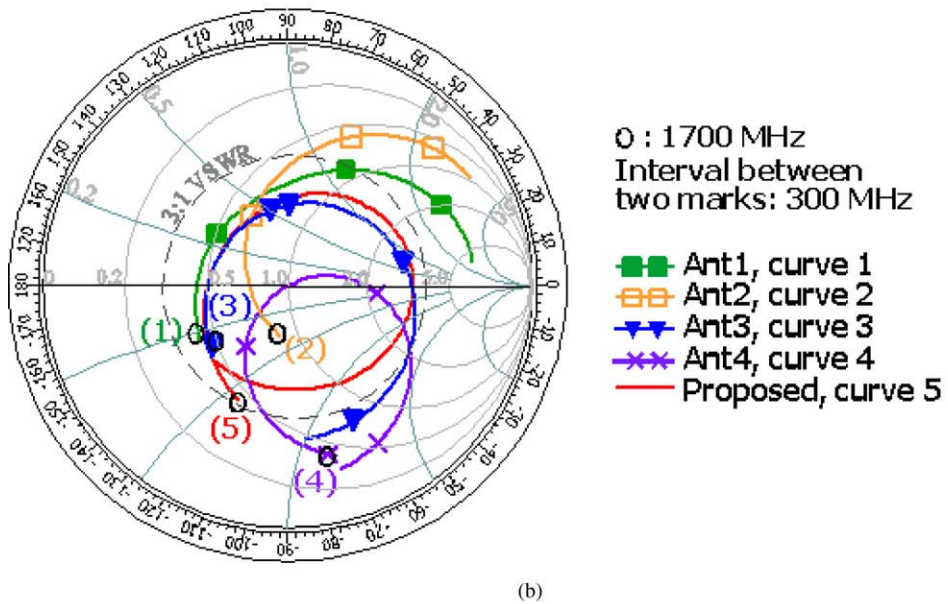
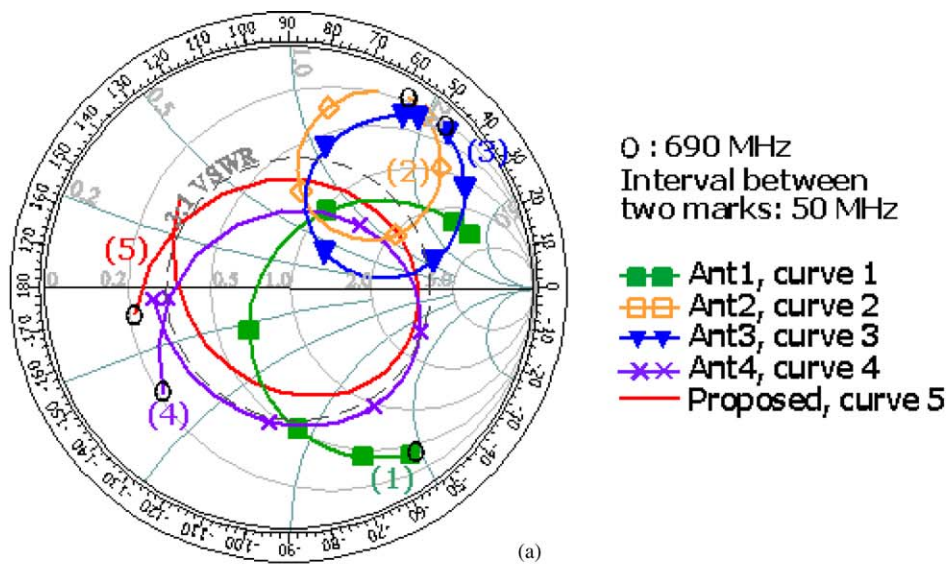


Figure 5 Simulated input impedance on the Smith chart for the proposed antenna without the wideband matching network (Ant1, curve 1), Ant1 with L_1 only (Ant2, curve 2), Ant1 with L_1 and C_1 only (Ant3, curve 3), Ant1 with L_1 , C_1 , and C_2 only (Ant4, curve 4), and Ant1 with L_1 , C_1 , C_2 , and L_2 (proposed antenna, curve 5). (a) Frequency range: 690–960 MHz and (b) frequency range: 1700–2700 MHz. [Color figure can be viewed in the online issue, which is available at wileyonlinelibrary.com]

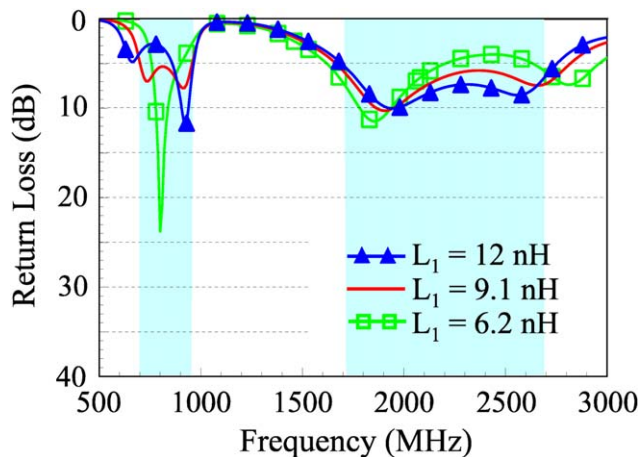


Figure 6 Simulated return loss as a function of L_1 for the proposed antenna. Other parameters are the same as in Figure 1. [Color figure can be viewed in the online issue, which is available at wileyonlinelibrary.com]

To analyze the effects of each element in the wideband matching network more clearly, Figure 5 shows the simulated input impedance on the Smith chart for the proposed antenna without the wideband matching network (Ant1, curve 1), Ant1 with L_1 only (Ant2, curve 2), Ant1 with L_1 and C_1 only (Ant3, curve 3), Ant1 with L_1 , C_1 , and C_2 only (Ant4, curve 4), and Ant1 with L_1 , C_1 , C_2 , and L_2 (proposed antenna, curve 5). In Figure 5(a), the results for the frequency range of 690–960 MHz are shown for analyzing the low-band performance, while the results for the frequency range of 1700–2700 MHz are shown in Figure 5(b) for analyzing the high-band performance.

Results show that when L_1 is added (see curve 1 vs. curve 2 in both Smith charts), curve 2 in Figure 5(a) becomes a loop-like curve, which indicates that dual-resonance behavior can be obtained for the antenna's low band. Also, relatively small effects on the high-band performance are seen. The effect of the shunt inductor L_1 is hence similar to that of a high-pass matching circuit.

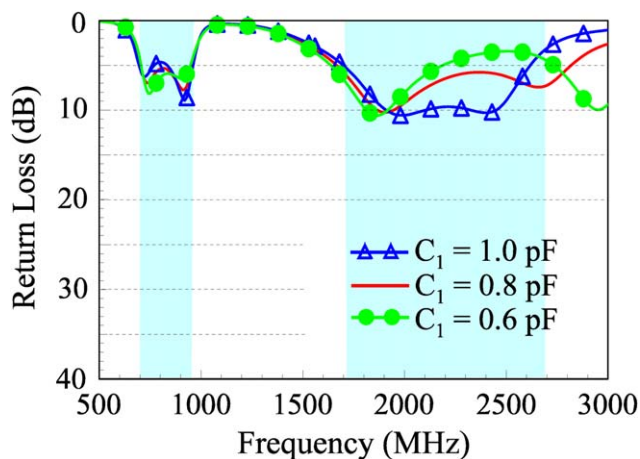


Figure 7 Simulated return loss as a function of C_1 for the proposed antenna. Other parameters are the same as in Figure 1. [Color figure can be viewed in the online issue, which is available at wileyonlinelibrary.com]

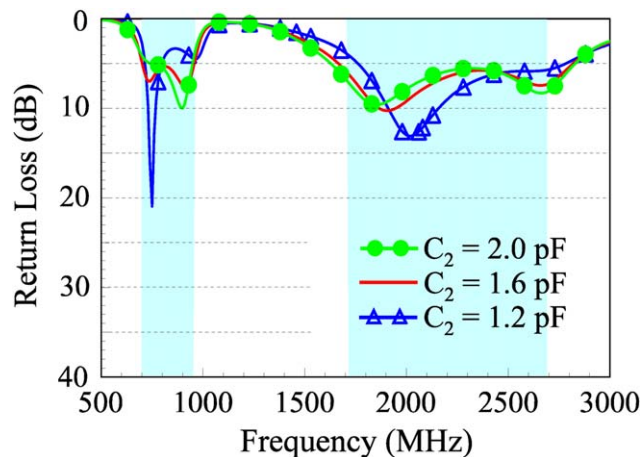


Figure 8 Simulated return loss as a function of C_2 for the proposed antenna. Other parameters are the same as in Figure 1. [Color figure can be viewed in the online issue, which is available at wileyonlinelibrary.com]

When C_1 is further added (see curve 2 vs. curve 3 in both Smith charts), curve 3 in Figure 5(b) becomes a loop-like curve, which also suggests that dual-resonance behavior can be obtained for the antenna's high band. Relatively small effects on the low-band impedance matching are also seen. In this case, the shunt capacitor C_1 has a similar effect as a low-pass matching circuit.

By further adding C_2 , curve 3 in Figure 5(a) can almost be shifted into the 3:1 VSWR circle as curve 4, and the antenna's low-band bandwidth is greatly widened. Conversely, the effect on the high-band performance is relatively small [see curve 3 vs. curve 4 in Figure 5(b)].

Finally, with L_2 added, small effects on the low-band performance are seen [see curve 4 vs. curve 5 in Figure 5(a)], while curve 4 in Figure 5(b) is seen to be shifted into the 3:1 VSWR as curve 5. In this case, the high-band bandwidth is greatly widened with L_2 added. The wideband matching network can hence lead to a dual-wideband operation for the antenna to cover the LTE low band (698–960 MHz) and high band (1710–2690 MHz).

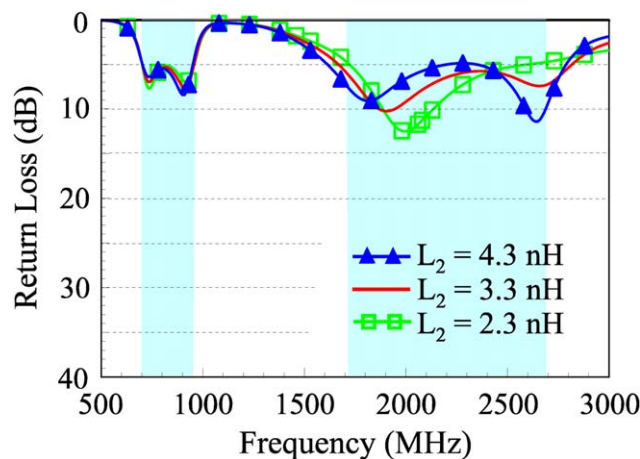


Figure 9 Simulated return loss as a function of L_2 for the proposed antenna. Other parameters are the same as in Figure 1. [Color figure can be viewed in the online issue, which is available at wileyonlinelibrary.com]

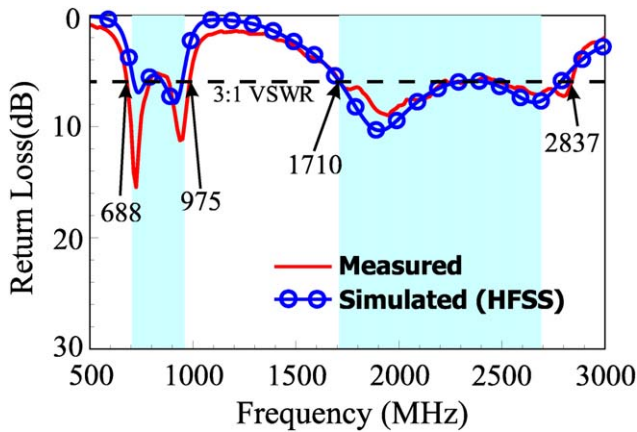


Figure 10 Measured and simulated return losses for the fabricated antenna. [Color figure can be viewed in the online issue, which is available at wileyonlinelibrary.com]

2.3. Parametric Study

In the wideband matching network, the inductor L_1 and capacitor C_1 are important in achieving dual-resonance behavior for the impedance matching of the antenna's low band and high band. That is, the impedance curve can become loop-like in the desired operating band. While the capacitor C_2 and inductor L_2 are mainly for shifting the loop-like impedance curve into the 3:1 VSWR circle. In this section, a parametric study on L_1 , C_1 , C_2 , and L_2 is presented. The simulated return loss as a function of L_1 for the proposed antenna is shown in Figure 6. Other parameters are the same as in Figure 1. Results for L_1 varied from 6.2 to 12 nH are presented. Results indicate that proper selection of L_1 is important in achieving good dual-resonance impedance matching for the antenna's low band. Conversely, relatively small variations in the antenna's high-band bandwidth are seen.

Figure 7 shows the simulated return loss as a function of C_1 for the proposed antenna. Results for C_1 varied from 0.6 to 1.0 pF are presented. Small effects on the antenna's low-band impedance matching are observed. Conversely, there are large effects on the dual-resonance behavior of the high band. This suggests that a proper selection of C_2 can lead to good dual-resonance behavior of the impedance matching of the antenna's high band, so that a widened high-band bandwidth can be obtained.

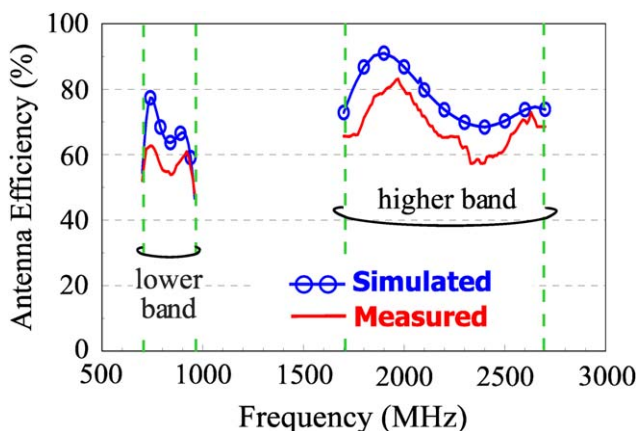


Figure 11 Measured and simulated antenna efficiencies (mismatching losses included) for the fabricated antenna. [Color figure can be viewed in the online issue, which is available at wileyonlinelibrary.com]

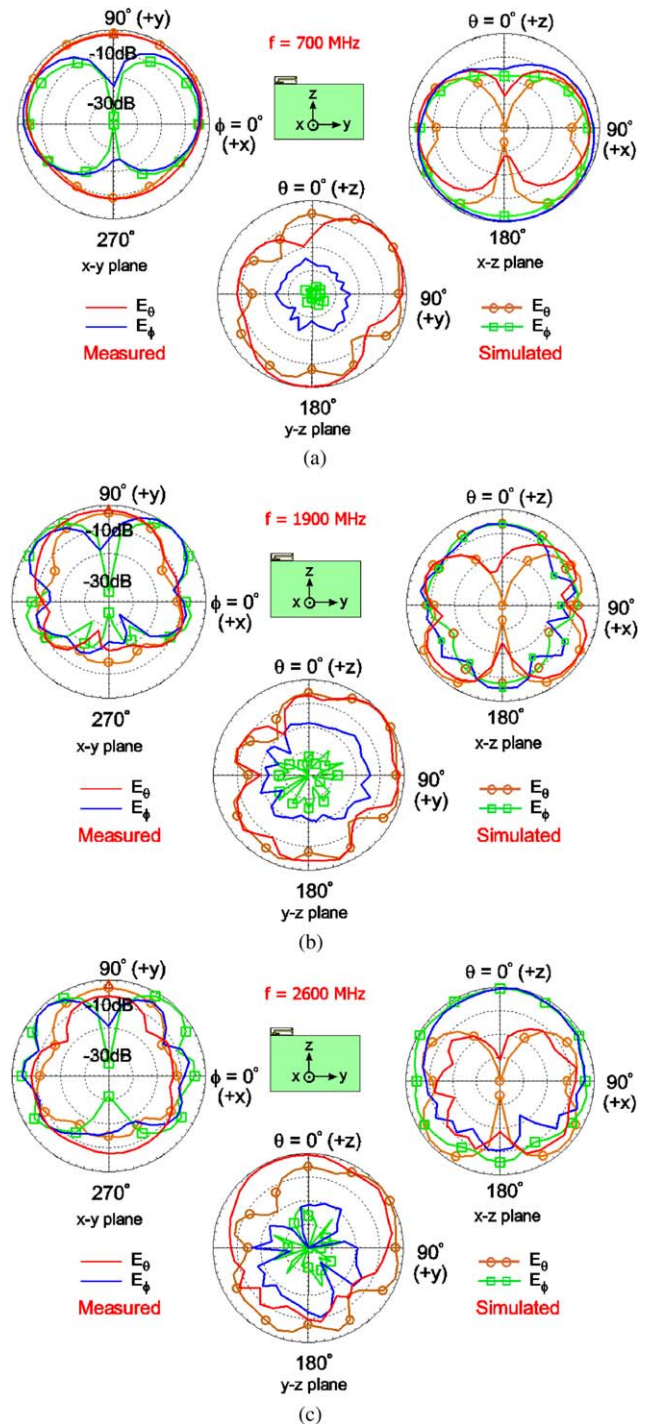


Figure 12 Measured and simulated radiation patterns for the fabricated antenna. [Color figure can be viewed in the online issue, which is available at wileyonlinelibrary.com]

Figure 8 shows the simulated return loss as a function of C_2 for the proposed antenna. Results for C_2 varied from 1.2 to 2.0 pF are presented. The variations in C_2 cause small variations in the antenna's high-band bandwidth. Conversely, large variations in the antenna's low-band bandwidth are observed. The results confirm the observation in Figure 5(a) that C_2 can lead to a widened bandwidth mainly for the antenna's low band.

Variations of L_2 on the impedance matching of the proposed antenna are shown in Figure 9. Results for L_2 varied from 2.3 to 4.3 nH are presented in the figure. It is seen that effects on the

antenna's low-band impedance matching are very small. Conversely, large effects on the high-band impedance matching are seen. This also confirms the observation in Figure 5(b) that L_2 can lead to improved impedance matching for frequencies in the antenna's high band.

3. EXPERIMENTAL RESULTS AND DISCUSSION

Photos of the fabricated antenna have been shown in Figure 2. The measured and simulated return losses for the fabricated antenna are presented in Figure 10. The measured data agree with the simulated results. The fabricated antenna can cover the LTE dual-wideband operation in the 698–960 and 1710–2690 MHz bands. The measured and simulated antenna efficiencies which include the mismatching losses are shown in Figure 11. The antenna is measured in a far-field anechoic chamber. The measured antenna efficiency reaches about 50–62% over the low band and is about 58–82% over the high band. The obtained antenna efficiencies are acceptable for practical mobile communication applications. Also note that the deviations between the measured and simulated antenna efficiencies may be owing to the ohmic losses of the lumped chip inductors and capacitors in the wideband matching network.

Figure 12 shows the measured and simulated radiation patterns at 700, 1900, and 2600 MHz for the fabricated antenna. The measured radiation patterns are seen to agree with the simulated results. Results in the principal planes of x - y (azimuthal plane), y - z plane (elevation plane parallel to the device ground), and x - z plane (elevation plane perpendicular to the device ground plane) are plotted for each representative frequency. The radiation intensities are normalized with respect to the same maximum intensity in all the three planes. At 700 MHz, the radiation pattern in the x - y plane is close to that of a dipole-like antenna. Strong radiation in the lower-half plane ($-z$ direction) of the x - z plane is also seen. These observations suggest that the device ground plane contributes to the radiation in the antenna's low band. Also, the asymmetric pattern seen in the y - z plane is mainly owing to the antenna mounted along the long edge and flushed to one corner of the device ground plane.

At 1900 and 2600 MHz, more variations are seen in the radiation patterns. At 2600 MHz, it is interesting to note that in the x - z plane, the radiation in the upper-half plane ($+z$ direction) is stronger than that in the lower-half plane ($-z$ direction). This behavior suggests that the device ground plane acts more like a reflector, which is different from that observed at 700 MHz. In general, the obtained radiation characteristics are similar to those of many reported LTE tablet computer antennas. No special distinctions are noted. This indicates that the proposed antenna will also be promising for tablet computer applications.

4. CONCLUSION

A simple tablet computer antenna design with the aid of an integrated wideband matching network to achieve the LTE dual-wideband operation in the 698–960 and 1710–2690 MHz bands has been proposed and experimental studied. The antenna is not only simple in structure, but also small in size. The occupied ground clearance in the tablet computer application is $10 \times 30 \text{ mm}^2$ only, and the antenna has a thin thickness of 3 mm. The working principle of the antenna, especially the effect of the wideband matching network on the antenna's dual-wideband operation has been addressed. Experimental results of the fabricated antenna have also been presented, and good radiation characteristics have been obtained. The proposed design can

provide a simple and easy way in implementing the LTE antenna with a small size for tablet computer applications.

REFERENCES

1. LTE Frequency Bands & Spectrum Allocations—a summary and tables of the LTE frequency band spectrum allocations for 3G & 4G LTE - TDD and FDD. Available at: <http://www.radio-electronics.com/>.
2. S.H. Chang and W.J. Liao, A broadband LTE/WWAN antenna design for tablet PC, *IEEE Trans Antennas Propag* 60 (2012), 4354–4359.
3. W.S. Chen and W.C. Jhang, A planar WWAN/LTE antenna for portable devices, *IEEE Antennas Wireless Propag Lett* 12 (2013), 19–23.
4. Y.L. Ban, S.C. Sun, J.L.W. Li, and W. Hu, Compact coupled-fed wideband antenna for internal eight-band LTE/WWAN tablet computer applications, *J Electromagn Waves Appl* 26 (2012), 2222–2233.
5. J.H. Lu and Z.W. Lin, Planar compact LTE/WWAN monopole antenna for tablet computer application, *IEEE Antennas Wireless Propag Lett* 12 (2013), 147–150.
6. K.L. Wong, H.J. Jiang, and T.W. Weng, Small-size planar LTE/WWAN antenna and antenna array formed by the same for tablet computer application, *Microwave Opt Technol Lett* 55 (2013), 1928–1934.
7. J.H. Lu and Y.S. Wang, Internal uniplanar antenna for LTE/GSM/UMTS operation in a tablet computer, *IEEE Trans Antennas Propag* 61 (2013), 2841–2846.
8. K.L. Wong and M.T. Chen, Small-size LTE/WWAN printed loop antenna with an inductively coupled branch strip for bandwidth enhancement in the tablet computer, *IEEE Trans Antennas Propag* 61 (2013), 6144–6151.
9. K.L. Wong and T.W. Weng, Small-size triple-wideband LTE/WWAN tablet device antenna, *IEEE Antennas Wireless Propag Lett* 12 (2013), 1516–1519.
10. K.L. Wong and T.W. Weng, Coupled-fed shorted strip antenna with an inductively coupled branch strip for low-profile, small-size LTE/WWAN tablet computer antenna, *Microwave Opt Technol Lett* 56 (2014), 1041–1046.
11. K.L. Wong and L.Y. Chen, Coupled-fed inverted-F antenna using an inverted-F coupling feed for small-size LTE/WWAN tablet computer antenna, *Microwave Opt Technol Lett* 56 (2014), 1296–1302.
12. P.W. Lin and K.L. Wong, Low-profile multibranch monopole antenna with integrated matching circuit for LTE/WWAN/WLAN operation in the tablet computer, *Microwave Opt Technol Lett* 56 (2014), 1662–1666.
13. K.L. Wong and T.W. Weng, Very-low-profile dual-wideband tablet device antenna for LTE/WWAN operation, *Microwave Opt Technol Lett* 56 (2014), 1938–1942.
14. P.W. Lin and K.L. Wong, Dual-feed small-size LTE/WWAN strip monopole antenna for tablet computer applications, *Microwave Opt Technol Lett* 55 (2013), 2571–2576.
15. K.L. Wong and L.Y. Chen, Small-size LTE/WWAN tablet device antenna with two hybrid feeds, *IEEE Trans Antennas Propag* 62 (2014), 2926–2934.
16. K.L. Wong and S.C. Chen, Printed single-strip monopole using a chip inductor for penta-band WWAN operation in the mobile phone, *IEEE Trans Antennas Propag* 58 (2010), 1011–1014.
17. T.W. Kang and K.L. Wong, Chip-inductor-embedded small-size printed strip monopole for WWAN operation in the mobile phone, *Microwave Opt Technol Lett* 51 (2009), 966–971.
18. K.L. Wong, T.W. Kang and M.F. Tu, Internal mobile phone antenna array for LTE/WWAN and LTE MIMO operations, *Microwave Opt Technol Lett* 53 (2011), 1569–1573.
19. C.H. Chang and K.L. Wong, Small-size printed monopole with a printed distributed inductor for penta-band WWAN mobile phone application, *Microwave Opt Technol Lett* 51 (2009), 2903–2908.
20. ANSYS HFSS. Ansoft Corp., Pittsburgh, PA. Available at: <http://www.ansys.com/products/hf/hfss/>.

© 2015 Wiley Periodicals, Inc.